Journal of
Synchrotron
Radiation

ISSN 0909-0495

Received 4 April 2005
Accepted 1 June 2005

Determination of the dynamic deformation tensor by time-resolved triple-crystal diffractometry

Yujiro Hayashi,[a,b]* Noboru Tsukuda,[c] Eiichi Kuramoto,[c] Yoshihito Tanaka[b,d] and Tetsuya Ishikawa[b]

[a]Interdisciplinary Graduate School of Engineering Sciences, Kyushu University, Kasuga, Fukuoka 816-8580, Japan, [b]SPring-8/RIKEN, Mikazuki, Hyogo 679-5148, Japan, [c]Research Institute for Applied Mechanics, Kyushu University, Kasuga, Fukuoka 816-8580, Japan, and [d]CREST, JST, Japan. E-mail: yhayashi@spring8.or.jp

Triple-crystal X-ray diffractometry has been combined with time-resolved measurement techniques. A simple time-resolved technique was employed by using a digital storage oscilloscope and a fast X-ray detector. The time dependence of the deformation tensor was determined for a gallium arsenide wafer after a flash of a 130 fs laser pulse. The laser pulse produced instantaneous expansion resulting in a localized convex surface. Time-resolved measurements showed that a flexural standing wave, explained well by the classical elasticity theory for thin plates, appeared in the relaxation process.

Keywords: triple-crystal diffractometry; time-resolved measurements; ultrashort-pulse laser; deformation tensor.

1. Introduction

Triple-crystal diffractometry (TCD) (Iida & Kohra, 1979; Fewster, 1989) has the capability of revealing in great detail small lattice deformations in almost perfect crystals. This is achieved by measuring the distribution of diffracted intensity in reciprocal space with high momentum resolution. The principle of the method is based on the fact that the lattice deformation is equivalently represented as a blur of intensity distribution around reciprocal lattice points. Therefore, using parallel and monochromatic incident X-rays to reduce instrumental blur, the Bragg diffracted beam from a sample crystal is angularly resolved by an analyzer crystal, usually made of a highly perfect crystal such as Si, thus obtaining the intensity distribution around the reciprocal lattice point. Highly brilliant X-rays from synchrotron light sources have helped to enhance the momentum resolution of TCD, and even allow triple-crystal topography (Kitano *et al.*, 1987).

The high brilliance of synchrotron radiation, on the other hand, has advanced time-resolved X-ray diffractometry for more than two decades (Helliwell & Rentzepis, 1997). Several time-resolving techniques, such as pump–probe, streak cameras and multichannel scaling, have been applied to the X-ray measurements according to the demanded time resolution and time range (Larsson *et al.*, 2002; Kawado *et al.*, 1989), although these techniques require specialized devices for fast X-ray detection and signal-processing circuits.

More-brilliant X-rays from undulators of third-generation synchrotron light sources have tempted us to combine TCD and time-resolved measurements in order to detect the slightest time-varying deformation in crystals. Consequently, we started developing time-resolved TCD (TRTCD) at the 27 m undulator beamline (BL19LXU) of SPring-8, which can, at the moment, deliver the brightest X-rays in the world (Hara *et al.*, 2002). As the first application of the combined technique, we have chosen the determination of a time-dependent deformation tensor of a semiconductor crystal excited by ultrashort laser pulses.

Ultrashort laser irradiation on a crystal generates localized heat which results in a localized bend with a convex surface symmetrical about the irradiation point (Li, 1990; Cheng *et al.*, 1994). This is called pulsed photothermal deformation (PPTD). PPTD and resulting dynamic deformation such as surface acoustic waves and Lamb waves have been investigated by time-resolved optical methods: reflectivity measurements (Thomsen *et al.*, 1986), probe beam deflection measurements (Sontag & Tam, 1985; Wright & Kawashima, 1992; Bennis *et al.*, 1998) and interferometric measurements (Wright *et al.*, 2001). These methods give integrated effects of deformation such as slope and displacement of the surface, but cannot directly determine a deformation tensor.

This paper describes the TRTCD application to the determination of the time-dependent deformation tensor of GaAs irradiated by 130 fs laser pulses. Accumulation of the output signals of a PIN photodiode detector in a digital storage oscilloscope served as a simple and easily obtainable time-resolving X-ray detection system, since both PIN detectors and digital storage oscilloscopes are available in most synchrotron radiation beamlines.

2. Experimental

The experiment was carried out using high-brilliant synchrotron radiation from the 27 m undulator at BL19LXU of SPring-8. In order to measure the distribution of diffracted intensity around a reciprocal lattice point of the sample crystal, TCD was set up as shown schematically in Fig. 1. The first double-Si(111) monochromator tuned the X-ray photon energy at 15 keV. The monochromated X-rays were incident on the second sample crystal, a (100) GaAs circular wafer of diameter 76 mm and thickness 0.63 mm, through a 0.1 mm × 0.1 mm slit. The sample was simply placed on a holder without any wax or glue, with [100] and [010] being parallel to the scattering plane. The 400 reflection from the sample with Bragg angle $\theta_B = 17.0^\circ$ was angularly analyzed by the third Si(111) analyzer crystal. The angles ω of the sample and θ of the analyzer were controlled using high-precision goniometers (Ishikawa *et al.*, 1992).

Reciprocal lattice points move with deformation. If we let axes x_1 and x_2 be parallel to [100] and [010], where the origin of the center of the surface is as shown in Fig. 1, a component $D_{11} = \partial u_1/\partial x_1$ of a deformation tensor is equivalent to the dilation of the spacing of (100), where u_i is the x_i component of the displacement. The dilation moves the reciprocal lattice point (400) in the direction of $[\bar{1}00]$. When the deformation is assumed to be uniform and small within the region illuminated by X-rays, the dilation is detected as a peak shift $\Delta\theta$ in a ω–2θ scan. The relation between D_{11} and $\Delta\theta$ is given by

$$D_{11} = -\Delta\theta/\tan\theta_B. \quad (1)$$

A shear component $D_{12} = \partial u_1/\partial x_2$ equivalent to the inclination of (100) in (010) is detected as a peak shift $\Delta\omega$ in an ω scan, since the inclination moves the reciprocal lattice point in the direction of $[0\bar{1}0]$. The relation between D_{12} and $\Delta\omega$ is given by

$$D_{12} = -\Delta\omega. \quad (2)$$

When the sample is irradiated by laser pulses, the dilation and the inclination vary with time. The time dependence is obtained from $\Delta\theta(t)$ and $\Delta\omega(t)$ given by measuring the time variation of diffracted intensity on every step of the ω–2θ scan and the ω scan. For time-resolved measurement of diffracted intensity a Si PIN photodiode detector (Hamamatsu, S3590-09) was used in photoconductive mode. The output from the photodiode was amplified 125 times by an amplifier (Stanford Research, SR240, 300 MHz). The amplifier output was averaged by a digital storage oscilloscope (Tektronix, TDS7104, 1 GHz) to give an averaged voltage signal. The output pulse duration of the photodiode determined the time resolution, 82 ns, of the measurement system. Although the storage ring provided X-ray pulses of duration 40 ps in every 23.6 ns, we could consider it quasi-continuous by asynchronous averaging over 10^4 times. The averaged voltage signal was found to be proportional to the X-ray intensity measured with an ionization chamber placed in front of the photodiode. The noise level of the averaged voltage was 1.3 mV, corresponding to 3.9×10^6 photons s^{-1} or 19 photons per synchrotron radiation pulse. Accordingly, the oscilloscope technique requires diffracted intensity with more than 10^7 photons s^{-1}. The technique is applicable to intense X-rays causing saturation of pulse count rates in multichannel scaling, and also effective for intense pulsed X-rays with a low repetition rate such as free-electron lasers.

The laser pulses irradiating the sample were generated from a mode-locked Ti:sapphire laser with a generative amplifier. The wavelength, pulse duration, energy, repetition rate and beam size of the laser were 800 nm, 130 fs, 7.5 mJ cm^{-2} $pulse^{-1}$, 1.0 kHz and 1.4 mm full width at half-maximum (FWHM) in diameter, respectively. The oscilloscope began time-resolved measurement of the diffracted intensity using output pulses of a laser detector, an avalanche photodiode (APD), as triggers. The time resolution and the full scale of the oscilloscope was set to 400 ns and 1 ms, respectively.

The time-resolved ω–2θ and ω scans were carried out at $x_2 = 0$ to which the laser pulses were guided. The time-resolved ω scans were also carried out at several positions on the x_2 axis outside of the laser beam. Thus, $D_{11}(t)$ at $x_2 = 0$ and $D_{12}(x_2, t)$ were obtained.

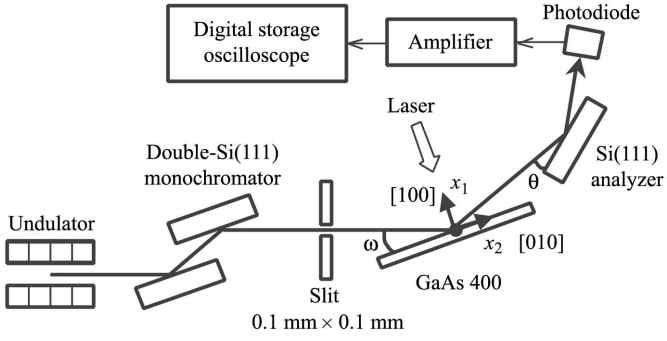

Figure 1
Experimental set-up for time-resolved triple-crystal diffractometry. The X-ray beam monochromated by the double-Si(111) monochromator was incident on a GaAs (100) sample wafer. The 400 reflection from the sample was detected through the Si(111) analyzer by a PIN photodiode in photoconductive mode. The output of the photodiode was amplified and then averaged by a digital storage oscilloscope.

3. Results and discussion

The dilation and the inclination characterizing PPTD were determined by TRTCD. The dilation, D_{11}, at $x_2 = 0$ to which the laser pulses were guided is shown in Fig. 2, which was obtained from the time-resolved ω–2θ scan profile shown in the inset. The inclination, D_{12}, at $x_2 = 0$ (*a*), −5 (*b*), 5 (*c*), −10 (*d*) and 10 mm (*e*) is shown in Fig. 3 with $t = 0$ being the time of laser shot. The full scale, 1 ms, of the time axis in Fig. 3 corresponds to one period of the laser repetition. The dilation at $x_2 = 0$ has a sharp rise at $t = 0$, followed by relaxation in 6 μs. The inclination at $x_2 = 0$ again has a sharp rise at $t = 0$, followed by relaxation in 0.2 ms. The inclination at the equidistant positions from $x_2 = 0$ has almost the same magnitude but opposite sign. Oscillating components of the inclination at $x_2 = \pm 5$ and ± 10 mm are found. The baselines of the oscillations at $x_2 = \pm 5$ mm are drawn by broken lines as guides for the eye as shown in Figs. 3(*b*) and 3(*c*). The baseline at $x_2 = -5$ and

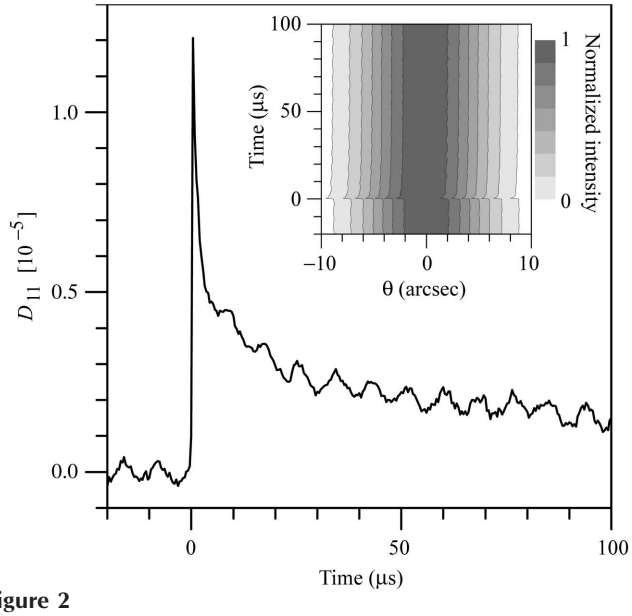

Figure 2
Time dependence of the dilation where $t = 0$ is the time of a laser shot. Inset: time-resolved ω–2θ scan profile.

+5 mm changes to positive and negative after a delay of several microseconds from $t = 0$, followed by relaxation in 0.3 ms, respectively. No significant changes of the baselines at $x_2 = \pm 10$ mm are found. The amplitudes of the oscillations at $x_2 = \pm 5$ and $\pm$ 10 mm remain unchanged for 1 ms.

PPTD dynamics are discussed from the dilation and the baselines of the inclination. First, the laser irradiation produced the rapid dilation and inclination at $x_2 = 0$. Here, no inclination should be at the laser irradiation point owing to the axial symmetry of the deformation, but there was the inclination at $x_2 = 0$, which indicates that the irradiation point deviated from $x_2 = 0$ by $\sim$0.1 mm. Secondly, the dilation and the inclination at $x_2 = 0$ started to relax immediately after the deformation. The difference in the relaxation time between the dilation and the inclination at $x_2 = 0$ can be explained as follows. The relaxation time of the dilation depends on the temperature gradient normal to the surface, which is determined by the 0.75 μm absorption length of the laser; that of the inclination depends on the lateral temperature gradient, which is determined by the laser beam profile. Since the latter was much larger than the former, the relaxation of the inclination was slower than that of the dilation. Thirdly, the positive and negative inclination at $x_2 = -5$ and 5 mm, shown by the baselines in Figs. 3(*b*) and 3(*c*), means a deformation with a convex surface. The several-microsecond delay of the baseline change is reasonable for the time that the transverse acoustic wave in the direction parallel to the surface takes for propagation by 5 mm. Last, no changes of the baselines at $x_2 = \pm 10$ mm show that the bend was localized in 20 mm.

Fourier analysis for the oscillations in Figs. 3(*b*)–3(*e*) showed that only the 8 kHz component was significant. This suggests that one of the resonance frequencies of flexural motion should be close to 8 kHz, since the periodic laser irradiation leads to the forced oscillations which are the harmonics of 1 kHz. The inclination fitted by an 8 kHz sinusoidal wave is plotted as a function of x_2/a at $t = -8, 0, 8, 16, 24, 32, 40$ and 48 μs in Fig. 4(*a*), where a is the radius of the wafer. The 8 kHz component of the inclination appears to be a flexural standing wave with five loops. The envelope of the waveform decreases as $|x_2|$ increases. It is to be noted that the deviation of the laser irradiation point from $x_2 = 0$ is negligible for the waveform with such a long wavelength.

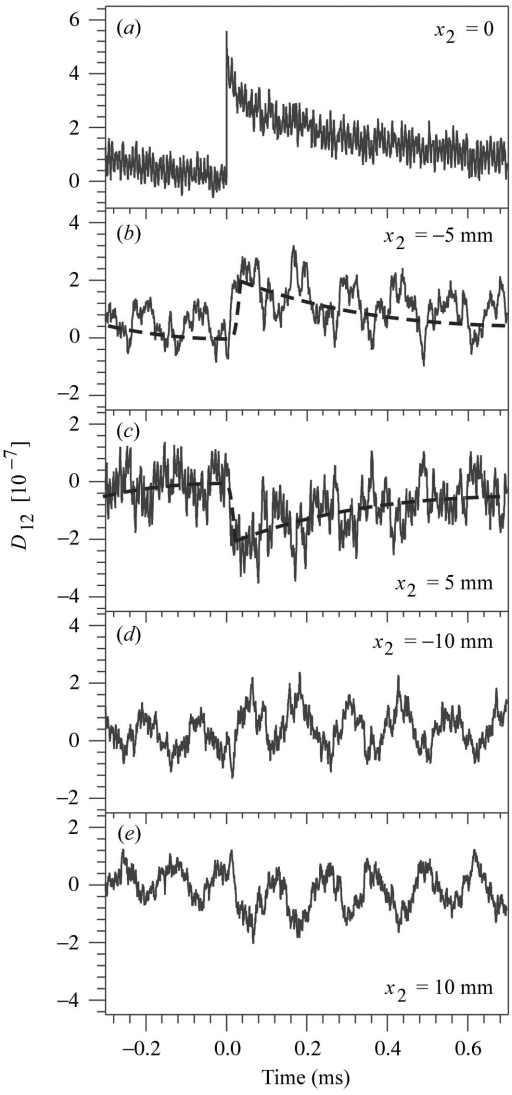

Figure 3
Time dependence of the inclination of the (100) plane at $x_2 = 0$ (*a*), −5 (*b*), 5 (*c*), −10 (*d*) and 10 mm (*e*). Baselines of oscillation in (*b*) and (*c*) are drawn by broken lines as guides for the eye.

Consider free flexural vibrations of a circular plate according to the classical elasticity theory for thin plates (Graff, 1991). The amplitude of the displacement of one of the modes is given by $AJ_0(kx_2) + CI_0(kx_2)$ in the cylindrical symmetry case about the x_1 axis, where J_n and I_n are the ordinary and modified Bessel functions of the first kind of order n, respectively (Leissa & Narita, 1980). Accordingly, the amplitude of the inclination for the mode is given by $-k[AJ_1(kx_2) - CI_1(kx_2)]$. The dispersion relation is $f = k^2hE^{1/2}/\{2\pi[3\rho(1 - \nu^2)^{1/2}]\}$, where f is the frequency, E is Young's modulus, ν is the Poisson ratio, ρ is the density and $2h$ is the

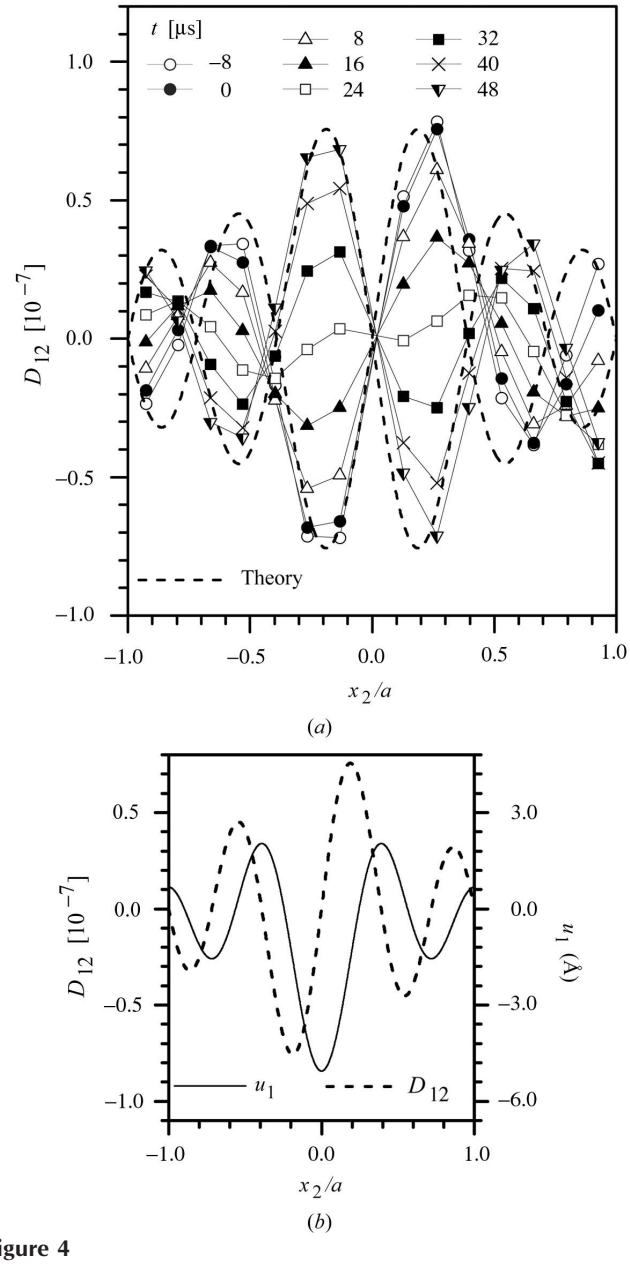

Figure 4
(*a*) The 8 kHz component of the inclination as a function of x_2/a at $t = -8$, 0, 8, 16, 24, 32, 40 and 48 μs. Broken lines show the amplitude of the inclination of a flexural standing wave calculated by the classical elasticity theory for thin plates. (*b*) Waveform of the displacement (solid line) derived from the calculation of the inclination (broken line) of the flexural standing wave at $t = 0$.

thickness of the plate. By inserting the E, ν and ρ values of Blakemore (1982) and the experimental result $f = 8$ kHz into the dispersion relation, the wavenumber k was estimated to be 2.6×10^2 m^{-1}. The amplitude ratio C/A is determined by the boundary condition. Since the sample was simply placed on the holder, the sample is assumed to be free on the circumference, *i.e.* the inclination is zero at $x_2 = a$. The amplitude of the inclination as a function of x_2/a is shown by broken lines in Fig. 4(*a*). The curve reproduces the experimental result with respect to the zero cross at $x^2 = 0$, the number of loops and the envelope.

Considering the phase term from Fig. 4(*a*), the inclination of the mode is expressed by $D_{12} = k[AJ_1(kx_2) - CI_1(kx_2)] \cos 2\pi ft$. Accordingly, the displacement is $u_1 = [AJ_0(kx_2) + CI_0(kx_2)] \cos(2\pi ft + \pi)$. The waveforms of the displacement and the inclination at $t = 0$ are shown in Fig. 4(*b*) by a solid line and a broken line, respectively. The amplitude of the displacement is less than 6 Å over 76 mm, as shown in Fig. 4(*b*). The displacement at $x_2 = 0$ is minimum at $t = 0$ and increases with time. Therefore, it is found that the laser irradiation has the function of raising the center to the surface side.

The observed deformation dynamics are summarized as follows. Laser pulse irradiation produced rapid expansion which made a localized bend with a convex surface symmetrical about the irradiation point. The periodic irradiation to the center of a circular wafer generated a cylindrical flexural standing wave driven by the impulsive force to the surface normal. The expansion and the bend started to relax immediately after the laser irradiation; the amplitude of the standing wave remained unchanged until the next laser irradiation.

4. Conclusion

We have developed a TRTCD at a brilliant undulator beamline at SPring-8 and applied it to the determination of the time-dependent deformation tensor of a GaAs wafer irradiated by 130 fs laser pulses. For time-resolved measurement, it was shown that the digital storage oscilloscope technique, whose time resolution is determined by the time response of a PIN photodiode detector, is useful when diffracted intensity is more than 10^7 photons s^{-1}. The technique is advantageous for intense X-rays causing saturation of photon count rates in counting techniques. The time-resolved measurements showed that a cylindrical flexural standing wave, explained well by the classical elasticity theory for thin plates, was excited in the relaxation process of laser-induced instantaneous expansion forming a localized convex surface.

This work was partially supported by a Grant-in-Aid from the Ministry of Education, Science, Sports and Culture of Japan.

References

Bennis, G. L., Vyas, R. & Gupta, R. (1998). *J. Appl. Phys.* **84**, 3602.
Blakemore, J. S. (1982). *J. Appl. Phys.* **53**, R123–R128.
Cheng, J. C., Wu, L. & Zhang, S. Y. (1994). *J. Appl. Phys.* **76**, 716–722.
Fewster, P. F. (1989). *J. Appl. Cryst.* **22**, 64–69.
Graff, K. F. (1991). *Wave Motion in Elastic Solids.* New York: Dover.
Hara, T., Yabashi, M., Tanaka, T., Bizen, T., Goto, S., Marechal, X. M., Seike, T., Tamasaku, K., Ishikawa, T. & Kitamura, H. (2002). *Rev. Sci. Instrum.* **73**, 1125–1128.
Helliwell, J. R. & Rentzepis, P. M. (1997). *Time-Resolved Diffraction*, ch. 5. Oxford University Press.
Iida, A. & Kohra, K. (1979). *Phys. Status Solidi A*, **51**, 533–542.
Ishikawa, T., Yoda, Y., Izumi, K., Suzuki, C. K., Zhang, X. W., Ando, M. & Kikuta, S. (1992). *Rev. Sci. Instrum.* **63**, 1015–1018.
Kawado, S., Kojima, S., Ishikawa, T., Takahashi, T. & Kikuta, S. (1989). *Rev. Sci. Instrum.* **60**, 2342–2345.
Kitano, T., Ishikawa, T., Matsui, J., Mizuki, J. & Kawase, Y. (1987). *Jpn. J. Appl. Phys.* **26**, L108–L110.

Larsson, J., Allen, A., Bucksbaum, P. H., Falcone, R. W., Lindenberg, A., Naylor, G., Missalla, T., Reis, D. A., Scheidt, K., Sjögren, A., Sondhauss, P., Wulff, M. & Wark, J. S. (2002). *Appl. Phys. A*, **75**, 467–478.
Leissa, A. W. & Narita, Y. (1980). *J. Sound Vib.* **70**, 221–229.
Li, B. C. (1990). *J. Appl. Phys.* **68**, 482–487.
Sontag, H. & Tam, A. C. (1985). *Appl. Phys. Lett.* **46**, 725–727.
Thomsen, C., Grahn, H. T., Maris, H. J. & Tauc, J. (1986). *Phys. Rev. B*, **34**, 4129–4138.
Wright, O. B. & Kawashima, K. (1992). *Phys. Rev. Lett.* **69**, 1668–1671.
Wright, O. B., Perrin, B., Matsuda, O. & Gusev, V. E. (2001). *Phys. Rev. B*, **64**, 081202.